Microfluidic Transport Driven by Opto-Thermal Effects

Matthieu Robert de Saint Vincent, Jean-Pierre Delville

1

Microfluidic Transport Driven by Opto-Thermal Effects

Matthieu Robert de Saint Vincent and Jean-Pierre Delville
Univ. Bordeaux, LOMA, UMR 5798, F-33400 Talence,
CNRS, LOMA, UMR 5798, F-33400 Talence
France

1. Introduction

Microfluidic applications to biology and chemistry rely on precise control over the transport of (bio-)molecules dissolved in tiny volumes of fluid. However, while the rigid environment of a microfluidic chip represents a convenient way to impose flows at the micrometer scale, an active control of transport properties usually requires the action of an external field (Squires & Quake, 2005).

Can light provide such control? Light indeed has several specific assets. First, as optical methods are contact-free, they are intrinsically sterile. Second, light fields can be tightly focused, providing by the way a very local and selective action. Third, light excitation can be totally disconnected from the chip (even though integration is possible (Monat et al., 2007)), therefore no microfabrication or specific treatment of the chip are required. This also provides a high degree of reconfigurability and versatility. The interest of applying optical fields to lab-on-a-chip devices is therefore evident.

Optical forces, which rely on the exchange of momentum between a light beam and a material object at a refractive index discontinuity (Ashkin, 1970), have led to the development of optical tweezers (Ashkin et al., 1986), themselves having opened a huge field of applications (Jonáš & Zemánek, 2008). However, the use of optical forces in the scope of microfluidic transport is limited by their very weak amplitude—typically, in the picoNewton range.

To circumvent this limitation, several alternatives have been proposed. The basic idea is to use light to induce hydrodynamic forces. A convenient means of doing this is to use a light source as a localized heater. The light beam thus provides a direct transfer of energy, rather than a transfert of momentum. Indeed, as the photon momentum equals its energy divided by the velocity of light, the total impulsion which can be communicated to an object is weak at given energy per photon. A direct transfer of energy therefore appears more favorable than a transfer of momentum to provide mechanical effects.

Besides the assets mentioned above, the use of focused light as a heating source has two extra advantages. On the one hand, it allows for producing very strong temperature gradients with a moderate heating. On the other hand, the possible disconnection from the chip, and the ability to duplicate or displace at will a laser beam (through galvanometric mirrors or holographic methods) provide two complementary ways of using the heating source: (i) a

'remote controlled' mode, in which the source is static, and (ii) a 'writing' mode, involving a continuously moving source. This complementarity opens the way to various opportunities.

How can the heating affect the transport properties of a fluid, or of a solute carried by this fluid? A first method consists in directly tuning the concentration of the solute, providing that the thermally-induced transport is strong enough to overcome the natural Brownian diffusion. Alternatively, the manipulation of the carrier fluid provides another way to control the transport of reagents. Such a manipulation can be achieved by tuning the fluid properties, density and viscosity, which are both temperature-dependent. On the other hand, diphasic flows are particularly relevant in lab-on-a-chip applications since they allow for the manipulation of calibrated volumes of reagents, while preventing from potential cross-contamination according to the immiscible character of the fluids involved (Song et al., 2006; Theberge et al., 2010). From the viewpoint of fluid manipulation, diphasic flows add another degree of freedom, namely, the interfacial tension, toward the control of fluid transport. Finally, a last possibility consists in performing phase changes, involving liquid-gas or gas-liquid transitions.

These two families of flows—mono- or diphasic flows—build the structure of the present chapter, basically constituting its two main parts, inside which we overview the main approaches developed in the literature. The scope of this review includes the transport of fluids and macromolecules of biological interest in the view of—proven or potential—lab-on-a-chip applications. Our purpose is not to give an exhaustive overview of the literature (especially, the manipulation techniques of small molecules, colloids, and nanoparticles, are not included in the present chapter), but rather to give a comprehensive survey, centered on the main physical mechanisms, and then to bridge the gap between the highly diverse opto-thermal approaches.

2. One-fluid flows

This section reviews the main transport phenomena involved in monophasic flows. We will first remind the main principles involved, then we will show two major research directions combining these methods, namely, the generation of channel-free microfluidic flows, and the manipulation of biological molecules.

2.1 Basic principles and methods

Three basic mechanisms, as summarized in Fig. 1, are involved in monophasic solutions: thermophoresis, thermal convection, and thermoviscous expansion. A more anecdotic alternative, involving a thermally-induced sol-gel transition, will also be briefly presented.

2.1.1 Thermophoresis

Thermophoresis, also called thermodiffusion, or Ludwig-Soret effect, takes place in solutions submitted to a temperature gradient (Piazza & Parola, 2008; Würger, 2010). The macroscopic effect is the creation, at steady state, of a concentration gradient overtaking the natural smoothing due to the Brownian diffusion (Fig. 1(a)). While this effect has been discovered in the mid-nineteenth century (independently by Ludwig and Soret), its theoretical

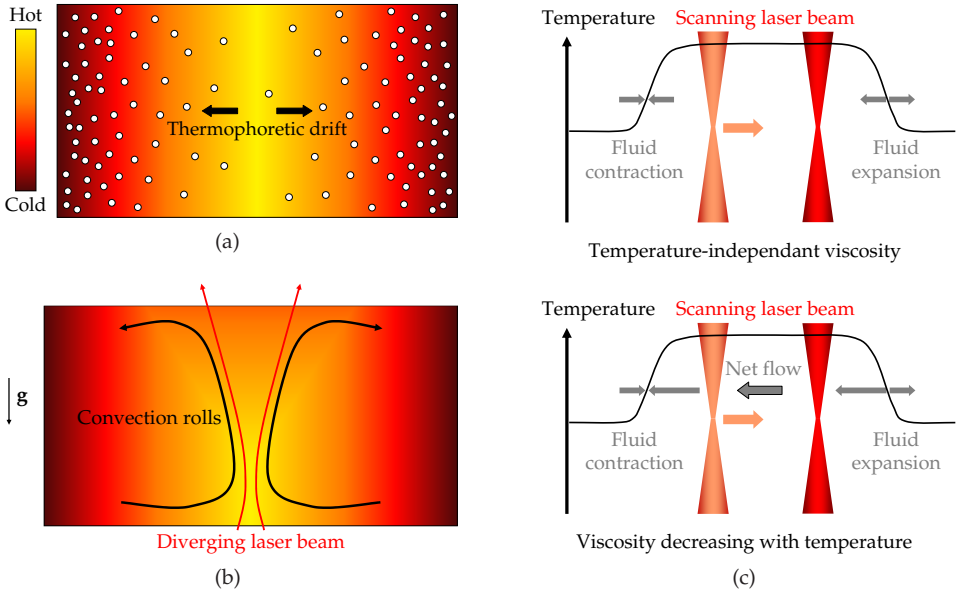

Fig. 1. Schematic illustration of the three main mechanisms involved in monophasic opto-thermal transport. (a) Thermophoresis of (here thermophobic) molecules, (b) laser-induced convection, and (c) thermoviscous expansion (adapted after Weinert & Braun (2008b)).

understanding is still controversial. The recent review by Würger (2010) provides significant insight on the different mechanisms which can be involved.

From a phenomenological point of view, the motion of particles submitted to a temperature gradient can be described as a thermophoretic drift of velocity

$$\mathbf{u}_{\text{Soret}} = -D_T \boldsymbol{\nabla} T, \tag{1}$$

with D_T the thermophoretic mobility. Note that the word 'particle' should be understood here in a generic meaning, including both molecules, nanoparticles, microbeads, etc. Indeed, while biomolecules will mainly be considered in the following, thermodiffusion applies to a broad range of systems. Even though fundamental differences exist in the involved physical mechanisms (more details can be found in (Würger, 2010)), the phenomenological description we provide here keeps its generality.

Comparing thermophoresis to the Brownian diffusion leads to the definition of the Soret coefficient,

$$S_T = \frac{D_T}{D}, \tag{2}$$

with D the Brownian diffusivity. This coefficient has the dimension of the inverse of a temperature. It can be either positive or negative and then determines both the direction and amplitude of the overall particle drift. To date, no unified theory is able to predict either the sign or the order of magnitude of the Soret coefficient, which have been observed to

usually depend on both solute and solvent parameters, as well as external conditions such as temperature (Piazza & Parola, 2008; Würger, 2010). The theoretical background aiming at describing the fluidic thermophoresis is built upon two main approaches. On the one hand, hydrodynamic descriptions rely on the hypothesis of quasi-slip flow at the particles boundary (Weinert & Braun, 2008a; Würger, 2007). On the other hand, at the microscopic scale, thermodynamic approaches assume the local thermodynamic equilibrium to account for solvent diffusivity and fluctuations (Duhr & Braun, 2006b; Würger, 2009).

A positive value of the Soret coefficient thus corresponds to a migration toward the colder regions ('thermophobic' behavior, as shown on Fig. 1(a)). Conversely, a solute with a negative Soret coefficient will be said 'thermophilic'. For DNA in aqueous buffer solution Braun & Libchaber (2002) measured $S_T = 0.14\ \mathrm{K}^{-1}$ at room temperature, but this coefficient has been observed to change of sign with temperature (Duhr & Braun, 2006b).

From an experimental point of view, the study of thermophoresis requires (i) to apply a temperature gradient to the test cell, and (ii) to detect and measure the resulting concentration distribution. Optical methods are indeed well suited to fulfill these two requirements. First, as already pointed out, a much higher temperature gradient can be produced by direct laser heating of the fluid than by externally heating the cell boundary. Second, the same laser beam can also be used to characterize the concentration gradient. One possible method relies on the thermal lensing effect: as the concentration gradient created by thermal diffusion modifies locally the refractive index of the solution, the transmitted beam is either focused or spread (effect called 'Soret lens'), depending on the direction of the solute migration (Giglio & Vendramini, 1974). An alternative method makes use of a fluorescent marker grafted to the particles of interest, or of the particles fluorescence themselves if applicable, to reconstruct the concentration profile in real time by microscope imaging (Duhr et al., 2004). Moreover, the temperature profile can also be monitored by using a temperature-dependant fluorescent marker.

2.1.2 Thermoconvection

Thermoconvection relies on the difference of density of an homogeneous fluid heated inhomogeneously. As density usually decreases with temperature, the local heating of a fluid leads to its dilatation. Considering the heating induced by a collimated laser beam with radial symmetry, the thermal expansion would also be axisymmetric, and no net flow would appear even in the case where the laser beam moves. Inducing a net flow in this case would require to break the heating symmetry. This can be done if the laser beam is divergent, as shown in Fig. 1(b): the fluid more heated at the bottom side raises up by buoyancy, then loses its heat and falls down, creating convective rolls (Boyd & Vest, 1975). This mechanism, generally known as Rayleigh-Bénard convection, is involved in many processes at the macroscopic scale, ranging from the cooking of pasta to atmospheric currents. However, in the micrometer-scale, gravity is not the predominant force, and the heating symmetry breakup induced by gravity is rather limited because the Rayleigh number, which controls the convection onset, behaves as the cube of the heated layer width. In that sense, thermal convection is usually not relevant at this scale. Microfluidic applications of thermoconvection can nevertheless be developed provided that the sample is thick enough, or that the other forces (essentially, viscous or capillary) can be efficiently reduced.

2.1.3 Thermoviscous expansion

Another elegant means of breaking the heating symmetry to induce a net flow has recently been proposed by Weinert & Braun (2008b). This method relies on the temperature dependance of viscosity of the fluid submitted to a scanning heating beam (Fig. 1(c)).

Let us consider a confined fluid, in which the influence of gravity is negligible. We first assume that the fluid viscosity does not depend on temperature, as shown on the top part of Fig. 1(c). As the laser beam moves, the fluid at the front of the spot scanning expands due to its decrease in density while, on the other hand, the fluid at the rear of the spot scanning contracts as well. As this thermal expansion is a linear process, expansion and contraction balance, and no net fluid flow is produced.

Let us now add the temperature dependence of fluid viscosity. As viscosity usually decreases with temperature, the expansion and contraction processes will be favored in the heated regions, as shown on the bottom part of Fig. 1(c). This dissymmetry results in a net flow, directed in the direction opposite to the scanning.

As thermal diffusion is faster, by several orders of magnitude, than the fluid flow, the fluid warms and cools down in milliseconds, so scanning can be operated at rates in the kiloHertz range. The resulting pump velocity can be expressed in a simple manner, dropping a numerical prefactor of order unity, as (Weinert & Braun, 2008b)

$$\begin{aligned} u_{\text{thermoviscous}} &= \text{scanning velocity} \times \text{thermal expansion} \times \text{thermal decrease of viscosity} \\ &= -f\ell_{\text{th}}\alpha\beta T^2. \end{aligned} \tag{3}$$

In this expression f is the scanning rate, ℓ_{th} the heating spot length scale, T the temperature rise, $\alpha = (1/\rho)(\partial\rho/\partial T)$ and $\beta = (1/\eta)(\partial\eta/\partial T)$ the thermal expansion coefficient and temperature dependance with temperature, respectively. For water, $\alpha = -3.3 \times 10^{-4}$ K^{-1} and $\beta = -2.1 \times 10^{-2}$ K^{-1}, then considering a heating spot size of 30 μm, a scanning rate of 5 kHz and a temperature rise of 10 K lead to a pump velocity of 104 μm s^{-1}.

2.1.4 Thermally-induced sol-gel transition

An alternative way, inducing a local phase transition in the fluid, should also be mentioned. As the thermoviscous expansion presented above, this approach relies on a thermally-induced change in the fluid viscosity, but in the framework of a phase change. Krishnan et al. (2009) used a thermorheological fluid (water containing 15 % w/w of Pluronic F127, a tribloc copolymer) flowing in a channel including an absorbing substrate. The laser heating induced a reversible gelation of the fluid, resulting in the interruption of the flow. A flow switch without any moving part was then achieved. A similar approach was also used to perform fluorescence-activated cell sorting (Shirasaki et al., 2006).

2.2 Channel-free microfluidic flows

The direct manipulation of volumes of fluid allows for the controlled creation of arbitrary flows without the need of a rigid microfluidic channel. In particular, Weinert & Braun (2008b) have shown that flows can be driven along complex patterns by thermoviscous pumping (Fig. 2). As illustrated in Fig. 2(a), an infrared laser beam writing the words 'LASER PUMP' can

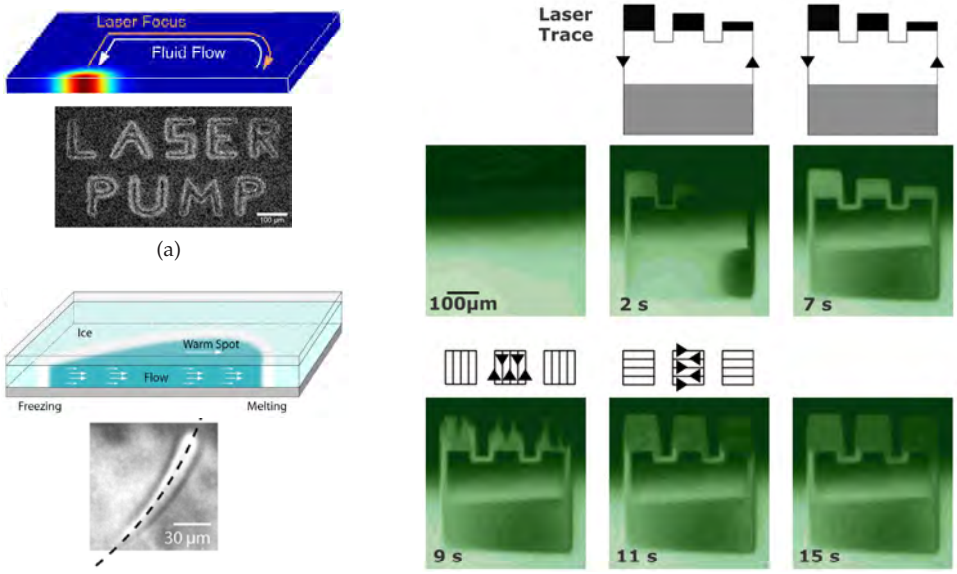

Fig. 2. Examples of channel-free flows performed by thermoviscous expansion. (a) A water flow is induced by a laser beam scanning in the opposite direction, and visualized by fluorescent tracer particles. From Weinert & Braun (2008b). (b) Thermoviscous motion in an ice sheet: the ice melts in front of the heating spot, and moves in the same direction due to the thermal expansion. The image is a superposition of frames of the molten spot along a curved path, shown in dashed line. From Weinert et al. (2009). (c) Optical creation of a dilution series of biomolecules. The system is composed of two neighboring gels, one of them (at the bottom) containing fluorescein-marked biomolecules. The laser beam first creates a liquid channel including three chambers of distinct volumes (upper panel), then mixes the content of these chambers with the ambiant fluid by pumping along a pattern alternating horizontal and vertical stripes. From Weinert & Braun (2008b).

produce a flow, in a 10-µm-thick water layer, in the direction opposite to the laser scanning. Due to the very small thickness of fluid involved, the thermoconvection cannot be invoked as a driving mechanism in this case.

The thermoviscous paradigm has also been extended to the case of melting ice (Weinert et al., 2009). In that particular case, the scanning laser first melts the ice, the liquid motion is then driven by thermal expansion, and finally the liquid refreezes (Fig. 2(b)). The motion can be described as a thermoviscous pumping in the case where the water does not freeze in the channel, when the chamber is cooled above 0°C. However, as the water density increases with temperature below 4°C the fluid flow takes same direction as the scanning. Pumping velocities of several cm s^{-1} can be reached.

The creation of fluid flows along arbitrarily complex patterns can, in principle, provide an alternative to the design of rigid dedicated channels. To highlight the potentialities of the method for (bio)chemical applications, Weinert & Braun (2008b) created a dilution series by

thermoviscous expansion. To this aim, they used a drop of agarose gel, gelated at room temperature, and molten by moderate heating (Fig. 2(c)). Biomolecules (30 kDa dextran marked with fluorescein) were added at the bottom part of the drop only, with a large amount of saccharose in order to avoid diffusion across the interface between the two halves of the gelated drop. The laser first draws a liquid channel along the two parts of the gel, creating in particular three liquid chambers of 65, 40, and 20 pL, respectively, in the upper part (initially without biomolecules). This step is represented in the upper row of Fig. 2(c). In a second step (lower row of Fig. 2(c)), the laser scans the gelated zones surrounding these chambers, along successive crossing lines. This scan enlarges the actual chambers, and dilute the biomolecules by mixing them with the molten agarose gel. As a result, a dilution series is created, with volume ratios of 4:1, 1:1, and 1:4 in equal volumes.

2.3 Manipulation of biological molecules: Diluting, trapping, replicating, and analyzing

Besides setting in motion a fluid, manipulating directly molecules of biological interest which might be dissolved in it is also of particular relevance. Such direct manipulation should indeed allow for precise tuning of the molecule concentration, and, further, for inducing particular reactions (especially, DNA replication).

2.3.1 DNA dilution or accumulation

As stated above, DNA exhibit a thermophobic behavior at room temperature (Braun & Libchaber, 2002). Therefore, the laser heating of a buffer solution of DNA deplete the zone at the vicinity of the spot due to the DNA thermophoretic drift, as illustrated in the right image of Fig. 3(a). Thermophoresis is therefore a convenient way of locally diluting a DNA solution. However, the most relevant issue is rather to concentrate molecules at a given point. Duhr & Braun (2006b) observed that the thermophoretic behavior of DNA could be reversed by simply cooling the sample: at 3°C, the DNA molecules become thermophilic and can therefore be trapped at the hot spot (left image of Fig. 3(a)). Besides this very simple method, several alternatives exist to perform effective DNA trapping.

One elegant way consists in opposing a liquid flow to the thermophoretic drift (Duhr & Braun, 2006a). This method seems particularly relevant in the lab-on-a-chip context due to its easy integrability into microfluidic channels. A 16-fold increase in DNA concentration was reached, at about 10 μm upstream from the beam axis, with a peak flow velocity of $0.55\ \mu m\,s^{-1}$. However, the time required to reach the equilibrium concentration profile is about 15 min, which limits the potentiality of the method for high-throughput applications.

By increasing the vertical temperature gradient effects, thermal convection can become significant. Figure 3(b) represents the effective DNA trapping by the interplay between these two mechanisms, as observed by Braun & Libchaber (2002). They considered a 50-μm-thick chamber, in the center of which a heating beam was focused. The top and bottom walls of the chamber were cooled to enhance the axial thermal gradient. The trapping mechanism is made of four main steps. First, the lateral thermophoresis drives the DNA molecules away from the heating spot (step 1). Then, the convection rolls carry the molecules downward, as the upward part of the rolls occur in the depleted zone close to the beam axis (step 2). The axial thermophoresis holds the DNA molecules at the chamber floor (step 3), where they finally accumulate at a radial position which result from the balance between lateral thermophoresis

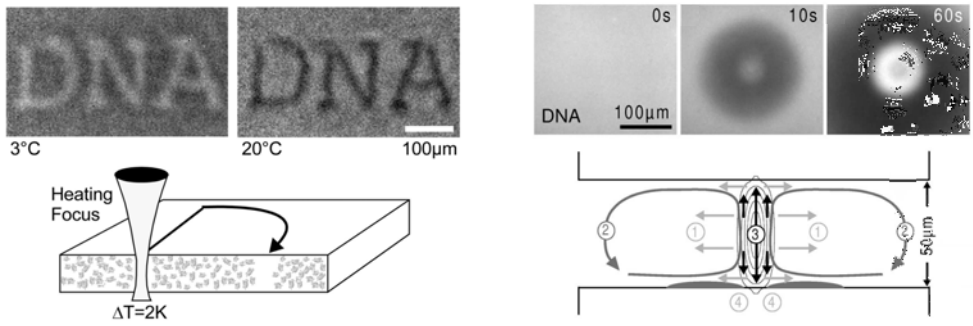

(a) (b)

Fig. 3. Optothermal dilution and trapping of DNA. (a) Use of the temperature dependance of the Soret coefficient to write complex DNA-enhanced or DNA-depleted patterns. When the microfluidic chamber is cooled down to 3°C the DNA molecules are thermophilic (left picture), while they are thermophobic at room temperature (right picture). From Duhr & Braun (2006b). (b) DNA trapping by a combination of thermophoresis and thermoconvection. From Braun & Libchaber (2002).

and convection (step 4). The DNA molecules are therefore trapped in a ring-shaped pattern around the laser beam axis. Braun & Libchaber (2002) observed a 60-fold local increase in concentration at steady state, which is reached within 60 s, for a mean temperature of about 80°C in the chamber. They even increased significantly the trapping efficiency, by using a thicker chamber (500 µm) and a divergent laser beam, in a scheme comparable to that represented in Fig. 1(b). The enhancement of the convection effect compared to the lateral thermophoresis leads to a point-like trapping pattern along the beam axis. After 180 s, a concentration increase by a factor of 2,450 was measured (Braun & Libchaber, 2002).

Another interesting trapping mechanism involves the combination of thermophoresis and a bidirectional flow induced by thermoviscous expansion in a very thin (2 µm) liquid layer (Weinert & Braun, 2009). Let us consider a vertical slice of this liquid layer, along the scanning path of the laser beam. As the laser scans, say, from the right to the left, then the lower part of the fluid will flow from the left to the right. However, the mass conservation applied together with lateral boundary conditions impose a symmetric counterflow in the upper part of the slice. Let us now reproduce at high rate the same scanning pattern, in such a way that each slice draws a radius of a circular fluid pancake, as illustrated in Fig. 4(a). The resulting flow pattern is therefore a toroidal roll, with a centrifugal flow at the bottom of the cell, and its centripetal counterpart at the top. In the meantime, the vertical temperature gradient drives the DNA molecules upward by thermophoresis. It means that the centrifugal flow concerns rather DNA-depleted fluid, while the centripetal flow advects more DNA molecules toward the center, where they accumulate.

As the scanning pattern is radial, the average trapping position is stationary. However, it can be still moved by displacing the average position of the scanning laser, allowing to collect particles over longer ranges. The so-called optothermal conveyor has been demonstrated efficient with small beads as well as DNA molecules (Fig. 4(b)).

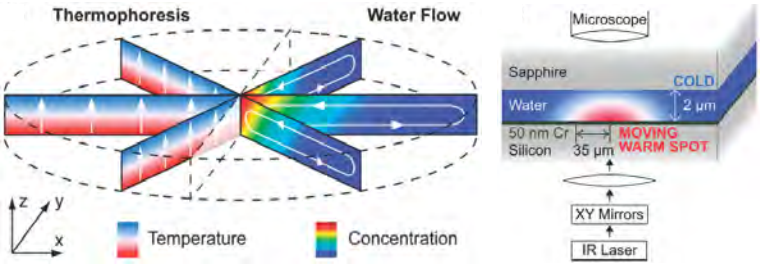

(a)

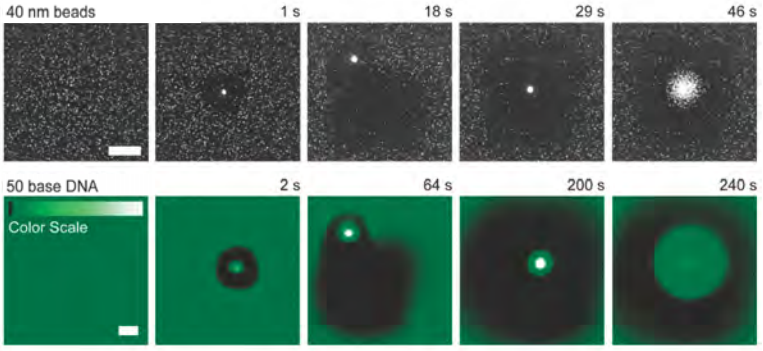

(b)

Fig. 4. Optothermal molecule conveyor (Weinert & Braun, 2009). (a) A radial centripetal laser scanning leads to the efficient trapping of molecules by a combination of thermophoresis and thermoviscous flow. The heating is provided at the bottom surface of the chamber by the laser absorption by a thin chromium coating. Typical warm spot radius is 35 µm. (b) Optical conveyor: the optothermal trap is moved along arbitrary patterns in order to collect particles (40 nm polystyrene beads, top row) or DNA molecules (bottom row, DNA concentration is given in color scale). After the laser has been switched off, the trapped objects are released and diffuse freely (right frames). The scale bars are 100 µm.

2.3.2 DNA replication

The investigations reported above highlight the possibility of DNA accumulation by purely thermal mechanisms. On the other hand, thermal convection has been shown to be able to drive the replication of DNA. The most popular DNA replication mechanism used by molecular biologists is polymerase chain reaction (PCR). Basically, each DNA molecule first dissociates into two single strands when heated at 95°C. In a second step (in the 55-65°C temperature range), pairs of short DNA fragments called primers, exhibiting sequences complementary to that to be amplified, anneal at the end of each single strand. Each of the two so-generated double helices finally elongate, by enzyme-activated replication of the complementary part of the initial strand (72°C). The process is then repeated cyclicly, each reaction cycle doubling the concentration of DNA exhibiting the targeted sequence. As pointed out by Braun et al. (2003), DNA molecules carried along a circular convection streamline experience a cycling change in temperature which mimic the temperature pattern

of a PCR. Mast & Braun (2010) then combined the trapping (by thermoviscous expansion and thermophoresis) and convective replication mechanisms in a capillary. Beyond the biotechnological interest of such a combination, it opens new perspectives for fundamental studies on the molecular evolution of life. Indeed, the two pillars on which the Darwinian evolutional theory relies, namely, the duplication of genetic material, and its storage against molecular diffusion, are retrieved. Moreover, inhomogeneously heated microfluidic chambers can be viewed as model systems reproducing the pores of hydrothermal rocks in the deep oceanic floor, in which life could have originated (Braun & Libchaber, 2004).

2.3.3 Analysis of biomolecular binding

Understanding the interactions between biomolecules, or between a particular biomolecule and its environment, is of crucial relevance for medical applications. Very recently, Braun and co-workers have proposed the use of thermophoresis as a probe of these interactions. As the thermophoretic properties of a solute depend on its interactions with the solvent (or, more generally, with its environment), they indeed proposed to quantify the biomolecular binding by accurately measuring the corresponding changes in thermophoretic depletion. This method has thus been used to quantify the aptamer-target interactions in a buffer solution (Baaske et al., 2010), and then generalized to various protein-protein and protein-ion binding in buffer solutions as well as in more complex biological liquids (Wienken et al., 2010).

2.3.4 Single molecule stretching

Besides the transport and analysis of DNA samples, several studies investigated the stretching of individual DNA molecules under the action of a laser-induced thermal gradient. Ichikawa et al. (2007) characterized the elongation of long DNA chains by the hydrodynamic stresses arising from thermal convection. Jiang & Sano (2007) anchored a DNA molecule by one or two ends and observed its deformation when located at a given distance from a heating laser. One-end-anchored molecules appear elongated along the direction opposite to the temperature gradient, while the two-end-anchored exhibit an arc-like shape when the laser is approached between the two bonded points. As the authors ensured the convection to be negligible, they interpreted the deformations to result from the thermophoretic drift of the movable parts of the molecule. From their observations, they calculated a tension force of about 70 fN for a 3 K μm^{-1} temperature gradient. These methods for studying the physical properties of biopolymers compete with others, such as AFM, optical or magnetic tweezers, by their contact- and probe-free characters.

3. Two-fluid flows

Let us now turn to the case of diphasic flows. We consider here, more generally, the case of a liquid droplet (a possible microreactor) immersed in, or floating on, another fluid, both of them being not miscible with each other. Controlling the microfluidic transport should here mean, essentially, controlling the motion of these microreactors. Then, hereafter is an overview of techniques to push, pull, divert, sort, or broadly speaking, manipulate droplets.

This section is divided into two parts. The first part deals with the direct manipulation of droplets through interfacial tension effects. The second one gathers different approaches involving one (or several) change(s) of state, in which at least two fluid phases are involved.

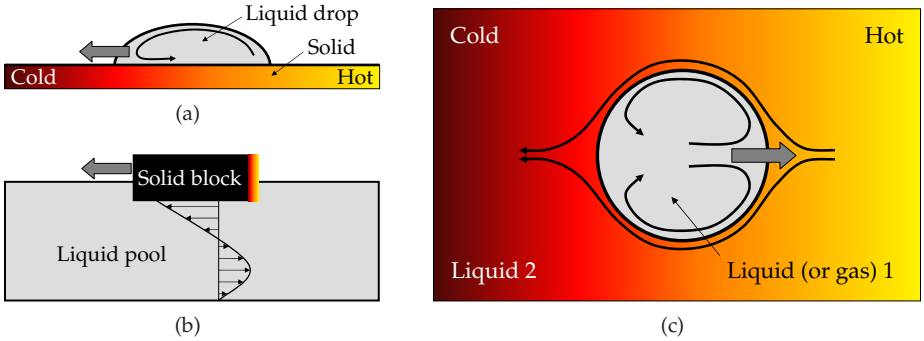

Fig. 5. Principle of thermocapillary migration, considering a surface (or interfacial) tension decreasing with temperature. (a) A liquid partly wetting a heated solid substrate is driven toward the colder regions by 'rolling' on the surface (as for a tracked vehicle). (b) A solid block floating on a liquid pool and heated at its end is propelled in the opposite direction (the schematic velocity field is in the laboratory frame). (c) An immersed droplet (or bubble) migrates to the warm by a 'swimming' motion.

3.1 Optocapillary effect

A spatial unbalance of surface tension along a liquid surface creates surface stresses. This effect, responsible for example for the phenomenon of 'wine tears', which can be observed above the free surface of wine in a clean glass, has been evidenced by Marangoni in 1871 and named after him. Over the past decade, this effect has known a renewed interest as it opens important vistas on the fluid manipulation at small scales. These potentialities are justified by the increased surface-to-volume ratio at small scales, which tends to favor interfacial effects compared to volume effects.

Basically, Marangoni effect appears as soon as a gradient of interfacial tension[1] is created, which can be achieved essentially through gradients of chemical composition or temperature. The resulting effect is then related as 'solutocapillary' or 'thermocapillary', respectively. For example, wine tears result from a gradient in ethanol concentration due to the excess evaporation in the rising wetting film, which increases the surface tension in these zones. Inhomogeneities in surfactant interfacial concentration can play the same role. Even though solutocapillary effect can be particulary relevant in microfluidic systems, this section will focus on thermocapillary effect—more precisely, 'optocapillary', i.e., thermocapillary effect in the special case where the temperature gradient is optically induced. Nevertheless, the role of surfactants can be significant, as we will see hereafter, to understand experimental features.

3.1.1 Thermocapillary migration: Basic principles

Creating an interfacial stress allows for setting in motion a fluid element (bubble, drop, liquid film), which we call thermocapillary migration, providing that a condensed surrounding medium can support this motion. For example, what follows would never happen if

[1] The term 'interfacial tension' is related to a liquid-liquid interface, when 'surface tension' is used for liquid-gas free surfaces. However, the phenomena presented in the following under the denomination 'interfacial tension' can be generalized to the free surface case.

considering a free levitating droplet in vacuum. Thermocapillary migration can therefore occur in the following cases, as reported in Fig. 5: a liquid element on a solid substrate (Fig. 5(a)), or conversely a solid element floating on a liquid surface (Fig. 5(b)), or a fluid element (either liquid or gas) in a liquid (Fig. 5(c)). In all cases considered here, the interfacial tension is supposed to decrease with temperature, so the driving temperature gradient leads to an inverted interfacial tension gradient—and therefore, interfacial stresses opposed to the temperature gradient.

In the first case (Fig. 5(a)), a partly wetting liquid drop is on an inhomogeneously heated substrate—note that the drop could as well be heated instead of the substrate. The surface stresses drive a surface flow at the droplet free surface, an opposite counterflow then results from mass conservation. Due to the no-slip condition at the solid-liquid boundary, this flow sets the drop in motion toward the high surface tension regions (Cazabat et al., 1990; Darhuber et al., 2003). Note that the particulary case of liquids on solid surfaces offers several additional degrees of freedom to spatially modulate the surface tension, including surface texturation, chemical patterning, or electrocapillarity. Further improvements can be found in the review by Darhuber & Troian (2005).

The symmetric case, less documented in the literature, involves an inhomogeneously heated solid, floating on a liquid surface (Fig. 5(b)). The surface stresses symmetrically drive the fluid on either sides of the hot point (creating a deeper counterflow as well). However, as the solid is heated from one side, the surface flow carries it toward the less heated direction.

The case of immersed bubbles (Fig. 5(c)) has been first treated half of a century ago by Young et al. (1959), then extended to droplets (Barton & Subramanian, 1989; Hähnel et al., 1989). It seems to be the most relevant to droplet microfluidic systems as no solid part is involved, avoiding any difficulty related to the liquid wetting (Chen et al., 2005). Here, the interfacial stresses drive an interfacial flow, in both sides of the interface, toward the colder part of the droplet. In the droplet, this flow creates internal rolls.[2] In the surrounding medium, this flow drags the bulk fluid, which in turn propels the droplet in the opposite direction according to the action-reaction principle. A simple analogy can be made with a swimmer, who drags fluid backward and then moves forward. Young et al. (1959) quantified the thermocapillary migration velocity of a bubble, and extended their calculation to droplets, in an infinite medium:

$$\mathbf{u}_{\text{thermocapillary}} = -\frac{2}{3\eta_1 + 2\eta_2} \frac{R}{2 + \Lambda_1/\Lambda_2} \frac{\partial \sigma}{\partial T} \boldsymbol{\nabla} T. \tag{4}$$

Here, R is the drop radius, Λ the thermal conductivity, and σ the interfacial tension. The subscripts 1 and 2 denote the droplet and surrounding phases, respectively. Considering a water droplet ($\eta_1 = 1$ mPa s and $\Lambda_1 = 0.6\ \mathrm{W\,K^{-1}\,m^{-1}}$), of radius 100 μm, in silicone oil ($\eta_2 \simeq 10$ mPa s and $\Lambda_2 \simeq 0.1\ \mathrm{W\,K^{-1}\,m^{-1}}$), with $\partial\sigma/\partial T \sim -0.1\ \mathrm{mN\,m^{-1}\,K^{-1}}$, a temperature gradient of $1\ \mathrm{K\,mm^{-1}}$ leads to a migration velocity of $110\ \mu\mathrm{m\,s^{-1}}$. This value rises up to $5\ \mathrm{mm\,s^{-1}}$ in the case of a gas bubble in water.

Beyond this ideal background, two main disturbing effects must be taken into account in microfluidic environments. First, the confining effect of channel walls would quantitatively

[2] The bubble case significantly differs: as gas is inviscid, the interfacial flow does not diffuse in the bulk gas phase, and then no flow is produced.

or qualitatively modify the physics of thermocapillary migration. Considering a squeezed bubble in a Hele-Shaw cell, Bratukhin & Zuev (1984) showed that the friction to walls reduces the migration efficiency, but the scaling $u_{\text{thermocapillary}} \sim -R\nabla T$ remains valid. The case of elongated bubbles in capillary tubes has then been treated both theoretically (Mazouchi & Homsy, 2000; 2001) and experimentally (Lajeunesse & Homsy, 2003). In the case of a polygonal cross-sectioned channel, they evidenced the strong influence of liquid flow through both corners and wetting films on the migration velocity. Especially, for a rectangular cross section the migration velocity then varies non-trivially with the channel aspect ratio, and no longer depends on the bubble size, due to the fluid recirculation through the corners. Furthermore, the recirculating flows through the wetting films add nonlinear corrections.

On the other hand, diphasic microfluidics often involves surfactants. Several investigations, both experimental (Barton & Subramanian, 1989; Chen et al., 1997) and theoretical (Kim & Subramanian, 1989a;b), have shown that insoluble surfactants tend to reduce the thermocapillary migration efficiency. A recent theoretical study by Khattari et al. (2002) has proposed to account for the surfactant effect by writing an 'effective' variation of interfacial tension with temperature, which for insoluble surfactants reads as

$$\left(\frac{\partial\sigma}{\partial T}\right)_{\text{eff}} = \left(\frac{\partial\sigma}{\partial T}\right)_{\Gamma} + \frac{\left(\frac{\partial\sigma}{\partial\Gamma}\right)_T}{\left(\frac{\partial^2\sigma}{\partial\Gamma^2}\right)_T}\left[\frac{1}{T}\left(\frac{\partial\sigma}{\partial\Gamma}\right)_T - \frac{\partial^2\sigma}{\partial T\partial\Gamma}\right], \tag{5}$$

with Γ the interfacial concentration. Although difficult to link with measurable quantities, the corrective term accounting for surfactant effect is expected to be positive as it reduces the effective variation of interfacial tension.

What was described above is related to thermocapillary effect in general. Let us now focus more specifically on optocapillary effect.

3.1.2 Optocapillary propelling

The three configurations depicted in Fig. 5 have been experimentally explored in an optocapillary scheme, as illustrated in Figs. 6 and 7.

The optocapillary migration of a liquid object (a film) on a heated solid surface is represented in Fig. 6(a). Garnier et al. (2003) considered an horizontal film, inhomogeneously heated by a light pattern which superimposes a gradient of intensity perpendicular to the contact line, and a sinusoidal intensity fluctuation along it. As a result, the contact line, mostly the less enlighten part, moves toward the darker edge, drawing the wavy-like pattern shown on Fig. 6(a). By varying the spatial periodicity of the illumination, the authors studied quantitatively the contact line instability.

Besides this study, relatively few publications are related to the optocapillary migration in the 'rolling droplet' configuration. However, this configuration is well adapted to the optical heating through surface plasmon decay (Farahi et al., 2005; Passian et al., 2006).

Thermocapillary migration of a solid floating object, within a scheme as represented in Fig. 5(b), is practically difficult to achieve since this requires the heating of a small movable object—heating the pool itself is however possible. Laser-induced heating is therefore a

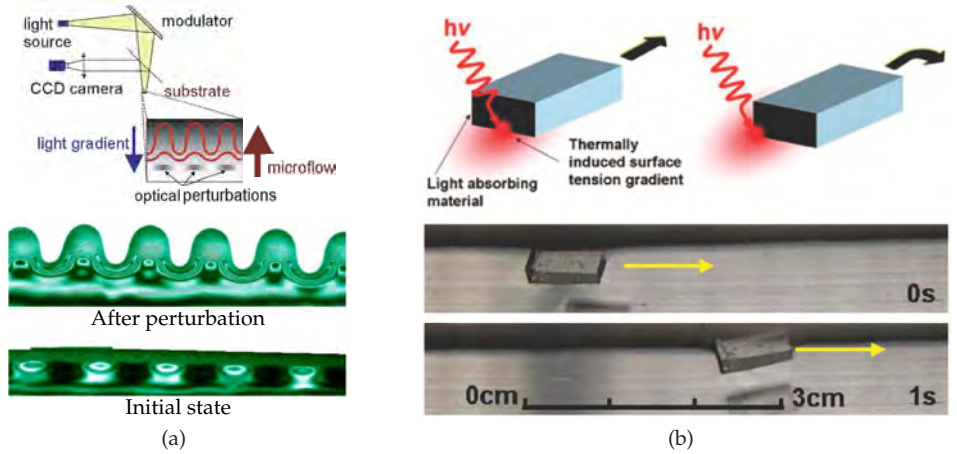

Fig. 6. Optocapillary migration at the liquid-solid boundary. (a) Migration of the contact line of an horizontal thin film induced by optical heating. The light intensity is spatially modulated in order to superimpose an horizontal light gradient perpendicular to the contact line and a sinusoidal fluctuation along it. Adapted from Garnier et al. (2003). (b) A millifluidic boat: a floating PDMS block, coated by an absorbent material at its back, is set in motion by light. Straight as well as turning motions can be achieved, depending on the irradiated point position compared to the object main axis. After Okawa et al. (2009).

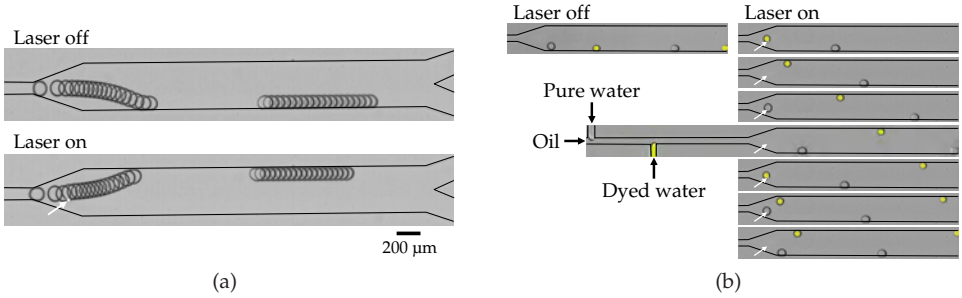

Fig. 7. Reverse optocapillary migration of immersed liquid droplets, in the presence of surfactants. (a) Superposition of frames showing droplet switching. Water droplets flowing in oil are optocapillary pushed away, and forced to flow through the upper part of the channel, of higher hydrodynamic resistance. (b) Application to droplet sorting: as water is transparent at the laser wavelength, droplets containing dye (colored on the frames) are diverted while pure water droplets are not. The white arrows depict the laser position. Adapted after Robert de Saint Vincent et al. (2008).

good solution as the focal point can follow the object motion. Okawa et al. (2009) realized a 'millifluidic boat' (Fig. 6(b)) by enlighting the back face of a PDMS block, coated with an absorbent material. The solid block then flow, at velocities up to the $\mathrm{cm\,s^{-1}}$ range, along remote-controlled trajectories, which can be either linear or curved depending on the relative location of the light spot in respect with the solid main axis.

As pointed out by the representation of Fig. 5(c), an immersed bubble should be attracted by the hot point. In the case of a laser heating, the bubble is trapped (Berry et al., 2000; Marcano & Aranguren, 1993), which implies that setting a bubble in permanent motion requires the laser to write this motion by moving the spot in the absorbing medium (Ohta et al., 2007). Rybalko et al. (2004) considered a slightly different case, in which an hemispherically-shaped absorbing droplet of nitrobenzene, floating on water, is alternatively shined at its front or at its back interface by simply changing the optical path from the above to the bottom part of the droplet. The resulting remote-controlled motion is alternatively forward and backward. Finally, another interesting alternative scheme has been presented recently by Nagy & Neitzel (2008), who set in levitation a laser-heated droplet above a solid substrate by using the thermocapillary flow to continuously feed the lubrication film. They were able to impose a translating motion to the drop, at velocities in the mm s^{-1} range.

The reversal of optocapillary motion has been reported in several recent studies (Baroud et al., 2007a; Dixit et al., 2010). While poorly understood yet, this reversal is expected to be related to the coupling between thermo- and solutocapillary effects. Indeed, eq. 5 suggests that the effective variation of interfacial tension with temperature could become positive provided that the term describing the influence of interfacial concentration is positive and larger than the pure temperature variation. However, answering decently this question would require much more complex calculations, involving coupled equations of heat and surfactant transport, which remain to date a numerical challenge.

As a consequence of this reversal, the thermocapillary migration is now oriented in such a way that a droplet is repelled by the heating light. This is illustrated in Fig. 7. Water droplets are carried by an oil flow in an enlarged channel with two outlets, and naturally flow through the lower outlet which has a lower hydrodynamic resistance. These droplets are passively diverted and then forced to flow through the other outlet by optocapillarity (Fig. 7(a)). This optocapillary effect is provided by heating the water droplets by a visible laser beam, a dye being added to the water to ensure light absorption. Such a scheme can be used to passively sort droplets on the basis of their optical properties (transparent or absorbent), as shown in Fig. 7(b). Considering alternate droplets of pure water and droplets containing dye (emphasized in color on the pictures), only the dyed droplets are diverted, while the others, which do not feel the laser heating, continue through the lower channel (Robert de Saint Vincent et al., 2008). Alternative applications, such as optocapillary pinball and conveyor, have also been demonstrated in the same view (Cordero et al., 2008).

3.1.3 Optocapillary blocking

In the case where $(\partial\sigma/\partial T)_{\text{eff}} > 0$, the laser beam can be viewed as a sort of 'soft wall' of tuneable stiffness. This ability to optically repel a droplet opens the way to the realization of optofluidic components (Baroud et al., 2007b). As represented in Fig. 8, the optocapillary blocking applied to a growing droplet in a flow focusing geometry (Anna et al., 2003) can interrupt the motion of the leading interface during several seconds. During the meantime, the water flow feeds the growing droplet. When eventually released, the blocked droplets are therefore larger than the unblocked ones, all the more so the blocking time has been long. Besides the ability to instantaneously interrupt a droplet flow, the optocapillary blocking of growing droplets provides a means of tuning in real time the droplet volume, by adjusting the blocking time via the beam power, without any action on the imposed flow parameters.

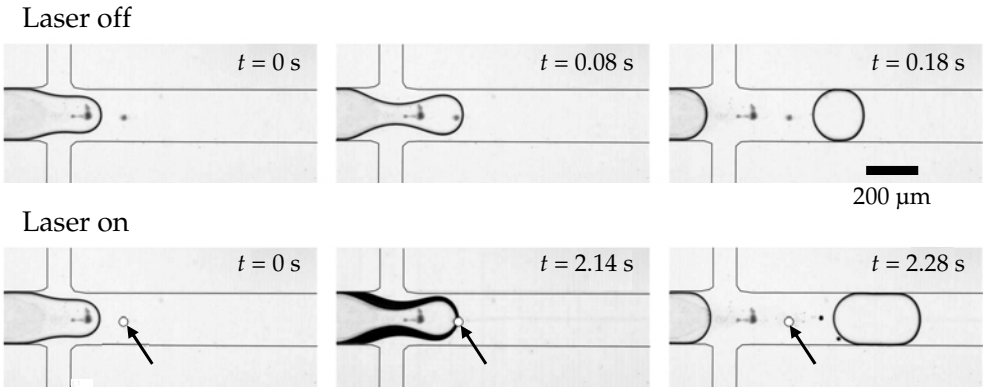

Fig. 8. Optocapillary blocking of the leading interface of an absorbent water droplet in oil during its formation. The picture representing the blocking process (lower row, center) is a superposition of 100 successive frames. The arrows depict the laser position. Adapted from Baroud et al. (2007a).

The optocapillary force exerting on a droplet during its blocking has been estimated theoretically (Baroud et al., 2007a) and experimentally (Verneuil et al., 2009) to be in the range of 0.1 µN with typical laser powers of 100 mW.

3.1.4 Splitting, merging and mixing

An important issue in the scope of application of droplets as microreactors is the ability of further controlling their volume and composition. This includes the calibration of droplets, to accurately adjust the quantity of reagents to be mixed, and the droplet coalescence. Both these operations have been performed optically (Fig. 9). First, calibrating the droplets can be done during their formation, as shown above (see Fig. 8). A subsequent modification of droplet volume would then require to split the droplet. Link et al. (2004) proposed a purely geometrical passive splitting scheme: a droplet arriving at a diverging junction splits into two equal or unequal parts depending on the hydrodynamic resistance (the length, in that work) of the diverging arms. The channel asymmetry can be reproduced, in a tunable way, by optocapillary repelling the droplet as it arrives at the T junction (Fig. 9(a)). A controllable part of the incoming droplet, depending on the beam power, is then forced to flow through the opposite channel (Baroud et al., 2007b). It has also been shown that, above a threshold power, the droplet is totally diverted and no longer splits.

Merging droplets is the symmetrical counterpart of the splitting operation. Due to the presence of surfactants, droplets are prevented from spontaneous coalescence. Interestingly, two very different approaches manage this issue—considering a $(\partial\sigma/\partial T)_{\text{eff}} > 0$ case in both. One consists in pushing a droplet toward a neighboring one, until contact, as represented on the top row of Fig. 9(b). The subsequent 'remote-controlled' merging is interpreted through the formation of a metastable bilayer surfactant film (Dixit et al., 2010; Kotz et al., 2004). The alternative approach consists in placing the laser spot at the interface that separates two contacting droplets (Baroud et al., 2007b). The bottom panel of Fig. 9(b) represents a train of contacting, noncoalescing droplets, flowing from the left to the right. Droplets then merge as

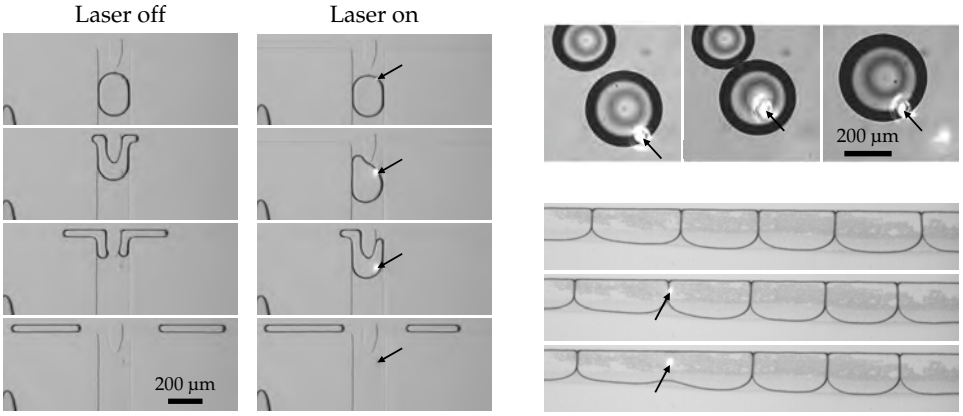

Fig. 9. Droplet splitting and merging. (a) Controlled splitting of droplet arriving at a symmetric T junction. The laser breaks the symmetry by reducing the water flow through the right channel. Adapted from Baroud et al. (2007b). (b) Optocapillary merging of droplets. Top row: the laser beam pushes a droplet away up to another droplet, then the two droplets coalesce (Dixit et al., 2010). Bottom panel: successive contacting droplets, flowing from the left to the right, are repeatedly merged when the interface is shined (Baroud et al., 2007b). The arrows depict the laser position.

the interface crosses the laser beam. Despite its reproducibility, this coalescing process remains misunderstood to date. In fact, Dell'Aversana et al. (1996) have shown, in an experimental scheme which can be viewed as comparable to that presented here, that thermocapillary flows have a preventing influence from coalescence, as the interfacial flow feeds the lubrication film which separates two contacting droplets. Therefore, while the film drainage could be possible in the 'remote-controlled' coalescence scheme where interfacial flows, directed toward the laser beam, drain the lubrication film off, the droplet coalescence in the flowing scheme is rather surprising.

Even though fusing droplets is a prerequisite to perform reactions in droplets, mixing the reagents after the merging is also necessary. However, in the microfluidic world mixing is unfavored due to the laminar character of the flows (low Reynolds number), which limits the advective mass transfers transversally to the main flow. Mixing would thus be driven by diffusion alone, requiring by the way unacceptably long times. Efficient mixing therefore requires a chaotic, 'stretching and folding', flow (Ottino & Wiggins, 2004).

As observed in Fig 5(c), thermocapillary stresses create rolls inside a droplet. Such rolls could be good candidates to perform effective mixing in microfluidic droplets (Grigoriev, 2005). However, the dipolar flow pattern created at steady state by a single heating source is not sufficient to induce mixing, as the streamlines do not intercross. A combination of dipolar and higher-order flows is thus required. By scanning a nanoliter droplet with a heating laser beam along a two-dimensional pattern, Grigoriev et al. (2006) induced chaotic mixing inside the droplet, through a combination of a bulk thermoconvective flow and an interface-driven thermocapillary flow. Cordero et al. (2009) used an optocapillary microdroplet blocking

scheme (see Fig. 8), combined with spatial and temporal light modulation techniques. They compared the mixing efficiency resulting from two stationary or one rapidly alternating heating beams and demonstrated that, despite the fact the spatial patterns are equivalent, only the non-stationary flow pattern produces mixing.

3.2 Flows induced by liquid-gas phase transitions

Up to now, we have essentially considered continuous changes on the fluid properties. Besides, we have also mentioned the specific use of phase transitions (namely, sol-gel transitions) to provide or prevent fluid motion when one fluid phase is involved. This section deals with phase transitions involving liquid and gas systems, applied to the generation or control of fluid motion. The two main approaches reported in the literature are presented in Fig. 10.

3.2.1 Successive evaporation-condensation cycles

A first approach consists in displacing tiny volumes of fluid by inducing successive cycles of evaporation-condensation-coalescence. Liu et al. (2006) considered a dilute solution of photothermal nanoparticles, which absorb light from a laser beam. As schematized on Fig. 10(a), the laser beam close to the leading edge of the liquid film first provides liquid evaporation. As the evaporated liquid cools down, it condensates and forms tiny droplets ahead the liquid film contact line. These droplets eventually coalesce and merge into the initial liquid film. This process results in an advance of the contact line: by repeating it after laser translation, a continuous flow can be obtained along the beam path. This flow can be guided laterally when the manipulation takes place in straight channels. Then, the laser can drive the fluid motion along a selected path, as illustrated in the experimental pictures in the right part of Fig. 10(a). Finally, the authors demonstrated the transport of Jurkat T-cells embedded in the solution.

Liu et al. (2006) experimentally obtained flows at velocities up to several hundreds of $\mu m\,s^{-1}$. According to the time required by the different mechanisms involved (heating, evaporation, condensation, coalescence, film advance), they estimated a maximal possible flow velocity of $1\,mm\,s^{-1}$.

Boyd et al. (2008) have recently proposed an alternative scheme involving the transfer of mass across a bubble in a partly filled microfluidic channel. A gas bubble is formed in the liquid phase, and a heating laser beam is focused in the liquid just behind the bubble. By slightly increasing the temperature at the rear of the bubble, the laser induces evaporation and the vapor then condenses at the front interface. This leads to a net fluid transfer across the bubble. The authors then applied this method to the distillation of a dye solution, the transferred solution being dye-free while the fluorescence enhancement can be observed in the untransferred one.

3.2.2 Flow actuation through bubble nucleation

The second phase transition-related approach is based on the nucleation of bubbles by laser. The simplest way of nucleating bubbles is to heat an absorbent fluid enough to reach the boiling point. Alternatively, a nonlinear process, called laser-induced cavitation, can be used

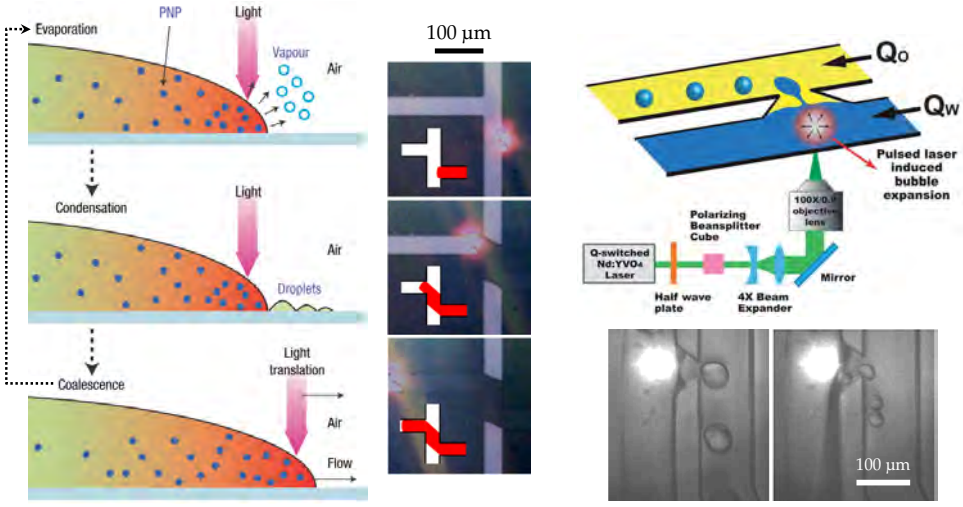

(a) (b)

Fig. 10. Phase transition-driven microfluidic flows. (a) A laser beam induces successive evaporation-condensation-coalescence cycles by heating a diluted photothermal nanoparticle (PNP) solution. The resulting fluid motion can follow complex paths inside a microfluidic channel (right pictures). Adapted from Liu et al. (2006). (b) Cavitation-induced droplet generation: a cavitation bubble created by a nanosecond pulsed laser expands and pushes a controlled volume of water into a parallel oil flow. Bottom pictures illustrate the produced bubbles, for pulse repetition rates of 0.5 (left) and 10 kHz (right, the three droplets shown here result from three successive pulses). Adapted from Park et al. (2011).

in transparent liquids (Vogel et al., 1989). The basic mechanism can be summarized as follows. A high-intensity light pulse is absorbed by an impurity contained in the transparent liquid, triggering optical breakdown. This creates a localized high-temperature and high-pressure plasma, which rapidly expands, resulting in shock wave emission and bubble formation. The bubble then grows and collapses in times in the millisecond range.

This bubble nucleation can be used to actuate fluid flows. Very recently, Park et al. (2011) used laser-induced bubble cavitation to trigger droplet formation in an oil flow in microfluidic channels. As represented in Fig. 10(b), water and oil flow in separated parallel channels, connected by a straight junction channel. A nanosecond pulsed laser, tightly focused in water close to this junction, induces cavitation bubble formation, which pushes water as it expands. The volume of water pushed in the oil channel is then dragged by the oil flow. By varying the pulse repetition rate, the authors produced monodisperse droplets at rates ranging from 0.5 up to 10 kHz. A comparable actuation process (while not involving the cavitation process) has also been proposed to eject particles or cells trapped in microfluidic traps, which is an elegant way of resetting trap-and-release-based microarray systems (Tan & Takeuchi, 2007; 2008). Finally, while not directly connected to fluid manipulation, biophotonics applications of laser-induced cavitation such as phototransfection (Stevenson et al., 2010) represent a current active research field.

4. Conclusions and prospects

Light fields represent a convenient and versatile tool to drive fluid transport by thermal effects. As seen in the present chapter, very different effects can be induced, involving either continuous changes in the fluid properties or phase transitions. The efficiency of opto-thermal effects, in addition to the specific assets of optical methods, set them as serious alternatives to non-optical microfluidic manipulation techniques—e.g. electric fields or microfabrication-based techniques. One key point in favor of these opto-thermal approaches is that they keep most of the advantages associated to the conventional optical manipulation techniques, without falling short of the high-throughput requirements in terms of force or velocity. The heating of the medium, sometimes relatively strong, can appear as a severe restriction, especially for biological application. However, as optical heating can be very localized, the inconvenience caused to the sample can be circumvent—or, at least, limited.

In addition, the diversity of opto-thermal approaches opens perspectives to cooperative effects. A good example is given by the optical conveyor, in which thermophoresis depletion of DNA and thermoviscous pumping, brought together, ultimately lead to the ability of trapping DNA at a position which can be changed at will. In the same way, the diverse complementary applications of optocapillary effect—blocking and propelling, splitting and merging—represent a good example of the high degree of versatility which can be reached by the same effect, when used in complementary means. Therefore, one can imagine that ultimately, light would be able to perform all operations relevant to lab-on-a-chip devices, ranging from sample preparation (dilution, concentration enhancement) to the final analysis (imaging and spectroscopy, which is beyond the scope of this review), including all steps associated with transport (sampling, carrying, sorting) and reactions (mixing). The optical lab-on-a-chip paradigm is furthermore compatible with droplet microfluidics.

From a more fundamental point of view, opto-thermal fluid manipulation techniques provide tools opening new perspectives in a broad field spectrum. One of the most exciting basic research directions for the next future is the investigation of prebiotic evolution of life, as suggested by the works of Braun and co-workers on thermally-driven DNA concentration and replication in microfluidic porous media. Still in the life sciences field, investigating biomolecular interactions, what has been proven a promising development for thermophoresis, is highly relevant for public health questions, as poorly-understood antigene-antibody interactions play a major role in medical treatments. Another direction is the investigation of biological and soft matter properties. This has been suggested, for example, by the investigations performed on single DNA molecule stretching by thermal convection, or submolecular thermodiffusion. Likely, optocapillarity provides a tool to investigate the behavior of interfaces submitted to strongly inhomogeneous stresses. Connexions could be found in relation with the study of breakup phenomena, which remains an active field of research since the second half of the nineteenth century.

5. References

Anna, S. L., Bontoux, N. & Stone, H. A. (2003). Formation of dispersions using “flow focusing” in microchannels, *Appl. Phys. Lett.* 82: 364–366.
URL: *http://link.aip.org/link/?APL/82/364/1*

Ashkin, A. (1970). Acceleration and trapping of particles by radiation pressure, *Phys. Rev. Lett.* 24: 156–159.
URL: *http://link.aps.org/doi/10.1103/PhysRevLett.24.156*

Ashkin, A., Dziedzic, J. M., Bjorkholm, J. E. & Chu, S. (1986). Observation of a single-beam gradient force optical trap for dielectric particles, *Opt. Lett.* 11: 288–290.
URL: *http://ol.osa.org/abstract.cfm?URI=ol-11-5-288*

Baaske, P., Wienken, C. J., Reineck, P., Duhr, S. & Braun, D. (2010). Optical thermophoresis for quantifying the buffer dependence of aptamer binding, *Angew. Chem. Int. Ed.* 49: 2238–2241.
URL: *http://dx.doi.org/10.1002/anie.200903998*

Baroud, C. N., Delville, J.-P., Gallaire, F. & Wunenburger, R. (2007a). Thermocapillary valve for droplet production and sorting, *Phys. Rev. E* 75: 046302.
URL: *http://link.aps.org/doi/10.1103/PhysRevE.75.046302*

Baroud, C. N., Robert de Saint Vincent, M. & Delville, J.-P. (2007b). An optical toolbox for total control of droplet microfluidics, *Lab Chip* 7: 1029–1033.
URL: *http://dx.doi.org/10.1039/B702472J*

Barton, K. D. & Subramanian, R. S. (1989). The migration of liquid drops in a vertical temperature gradient, *J. Colloid Interface Sci.* 133: 211–222.
URL: *http://dx.doi.org/10.1016/0021-9797(89)90294-4*

Berry, D. W., Heckenberg, N. R. & Rubinsztein-Dunlop, H. (2000). Effects associated with bubble formation in optical trapping, *J. Mod. Opt.* 47: 1575–1585.
URL: *http://www.tandfonline.com/doi/abs/10.1080/09500340008235124*

Boyd, D. A., Adleman, J. R., Goodwin, D. G. & Psaltis, D. (2008). Chemical separations by bubble-assisted interphase mass-transfer, *Anal. Chem.* 80: 2452–2456.
URL: *http://dx.doi.org/10.1021/ac702174t*

Boyd, R. D. & Vest, C. M. (1975). Onset of convection due to horizontal laser beams, *Appl. Phys. Lett.* 26: 287–288.
URL: *http://link.aip.org/link/?APL/26/287/1*

Bratukhin, Y. K. & Zuev, A. L. (1984). Thermocapillary drift of an air bubble in a horizontal Hele-Shaw cell, *Fluid Dyn.* 19: 393–398.
URL: *http://dx.doi.org/10.1007/BF01093902*

Braun, D., Goddard, N. L. & Libchaber, A. (2003). Exponential DNA replication by laminar convection, *Phys. Rev. Lett.* 91: 158103.
URL: *http://link.aps.org/doi/10.1103/PhysRevLett.91.158103*

Braun, D. & Libchaber, A. (2002). Trapping of DNA by thermophoretic depletion and convection, *Phys. Rev. Lett.* 89: 188103.
URL: *http://link.aps.org/doi/10.1103/PhysRevLett.89.188103*

Braun, D. & Libchaber, A. (2004). Thermal force approach to molecular evolution, *Phys. Biol.* 1: P1–P8.
URL: *http://stacks.iop.org/1478-3975/1/i=1/a=P01*

Cazabat, A.-M., Heslot, F., Troian, S. M. & Carles, P. (1990). Fingering instability of thin spreading films driven by temperature gradients, *Nature* 346: 824–826.
URL: *http://dx.doi.org/10.1038/346824a0*

Chen, J. Z., Troian, S. M., Darhuber, A. A. & Wagner, S. (2005). Effect of contact angle hysteresis on thermocapillary droplet actuation, *J. Appl. Phys.* 97: 014906.
URL: *http://link.aip.org/link/?JAP/97/014906/1*

Chen, Y. S., Lu, Y. L., Yang, Y. M. & Maa, J. R. (1997). Surfactant effects on the motion of a droplet in thermocapillary migration, *Int. J. Multiphase Flow* 23: 325–335.
URL: *http://dx.doi.org/10.1016/S0301-9322(96)00066-3*

Cordero, M. L., Burnham, D. R., Baroud, C. N. & McGloin, D. (2008). Thermocapillary manipulation of droplets using holographic beam shaping: Microfluidic pin ball, *Appl. Phys. Lett.* 93: 034107.
URL: *http://link.aip.org/link/?APL/93/034107/1*

Cordero, M. L., Rolfsnes, H. O., Burnham, D. R., Campbell, P. A., McGloin, D. & Baroud, C. N. (2009). Mixing via thermocapillary generation of flow patterns inside a microfluidic drop, *New J. Phys.* 11: 075033.
URL: *http://stacks.iop.org/1367-2630/11/i=7/a=075033*

Darhuber, A. A. & Troian, S. M. (2005). Principles of microfluidic actuation by modulation of surface stresses, *Annu. Rev. Fluid Mech.* 37: 425–455.
URL: *http://www.annualreviews.org/doi/abs/10.1146/annurev.fluid.36.050802.122052*

Darhuber, A. A., Valentino, J. P., Davis, J. M., Troian, S. M. & Wagner, S. (2003). Microfluidic actuation by modulation of surface stresses, *Appl. Phys. Lett.* 82: 657–659.
URL: *http://link.aip.org/link/?APL/82/657/1*

Dell'Aversana, P., Banavar, J. R. & Koplik, J. (1996). Suppression of coalescence by shear and temperature gradients, *Phys. Fluids* 8: 15–28.
URL: *http://link.aip.org/link/?PHF/8/15/1*

Dixit, S. S., Kim, H., Vasilyev, A., Eid, A. & Faris, G. W. (2010). Light-driven formation and rupture of droplet bilayers, *Langmuir* 26: 6193–6200.
URL: *http://dx.doi.org/10.1021/la1010067*

Duhr, S., Arduini, S. & Braun, D. (2004). Thermophoresis of DNA determined by microfluidic fluorescence, *Eur. Phys. J. E* 15: 277–286.
URL: *http://dx.doi.org/10.1140/epje/i2004-10073-5*

Duhr, S. & Braun, D. (2006a). Optothermal molecule trapping by opposing fluid flow with thermophoretic drift, *Phys. Rev. Lett.* 97: 038103.
URL: *http://link.aps.org/doi/10.1103/PhysRevLett.97.038103*

Duhr, S. & Braun, D. (2006b). Why molecules move along a temperature gradient, *Proc. Natl. Acad. Sci. USA* 103: 19678–19682.
URL: *http://www.pnas.org/content/103/52/19678.abstract*

Farahi, R. H., Passian, A., Ferrell, T. L. & Thundat, T. (2005). Marangoni forces created by surface plasmon decay, *Opt. Lett.* 30: 616–618.
URL: *http://ol.osa.org/abstract.cfm?URI=ol-30-6-616*

Garnier, N., Grigoriev, R. O. & Schatz, M. F. (2003). Optical manipulation of microscale fluid flow, *Phys. Rev. Lett.* 91: 054501.
URL: *http://link.aps.org/doi/10.1103/PhysRevLett.91.054501*

Giglio, M. & Vendramini, A. (1974). Thermal lens effect in a binary liquid mixture: A new effect, *Appl. Phys. Lett.* 25: 555–557.
URL: *http://link.aip.org/link/?APL/25/555/1*

Grigoriev, R. O. (2005). Chaotic mixing in thermocapillary-driven microdroplets, *Phys. Fluids* 17: 033601.
URL: *http://link.aip.org/link/?PHF/17/033601/1*

Grigoriev, R. O., Schatz, M. F. & Sharma, V. (2006). Chaotic mixing in microdroplets, *Lab Chip* 6: 1369–1372.
URL: *http://dx.doi.org/10.1039/B607003E*

Hähnel, M., Delitzsch, V. & Eckelmann, H. (1989). The motion of droplets in a vertical temperature gradient, *Phys. Fluids A* 1: 1460–1466.
URL: *http://link.aip.org/link/?PFA/1/1460/1*

Ichikawa, M., Ichikawa, H., Yoshikawa, K. & Kimura, Y. (2007). Extension of a DNA molecule by local heating with a laser, *Phys. Rev. Lett.* 99: 148104.
URL: *http://link.aps.org/doi/10.1103/PhysRevLett.99.148104*

Jiang, H.-R. & Sano, M. (2007). Stretching single molecular DNA by temperature gradient, *Appl. Phys. Lett.* 91: 154104.
URL: *http://link.aip.org/link/?APL/91/154104/1*

Jonáš, A. & Zemánek, P. (2008). Light at work: the use of optical forces for particle manipulation, sorting, and analysis, *Electrophoresis* 29: 4813–4851.
URL: *http://dx.doi.org/10.1002/elps.200800484*

Khattari, Z., Steffen, P. & Fischer, T. M. (2002). Migration of a droplet in a liquid: effect of insoluble surfactants and thermal gradient, *J. Phys.: Condens. Matter* 14: 4823–4828.
URL: *http://stacks.iop.org/0953-8984/14/i=19/a=309*

Kim, H. S. & Subramanian, R. S. (1989a). Thermocapillary migration of a droplet with insoluble surfactant: I. Surfactant cap, *J. Colloid Interface Sci.* 127: 417–428.
URL: *http://dx.doi.org/10.1016/0021-9797(89)90047-7*

Kim, H. S. & Subramanian, R. S. (1989b). Thermocapillary migration of a droplet with insoluble surfactant: II. General case, *J. Colloid Interface Sci.* 130: 112–129.
URL: *http://dx.doi.org/10.1016/0021-9797(89)90082-9*

Kotz, K. T., Noble, K. A. & Faris, G. W. (2004). Optical microfluidics, *Appl. Phys. Lett.* 85: 2658–2660.
URL: *http://link.aip.org/link/?APL/85/2658/1*

Krishnan, M., Park, J. & Erickson, D. (2009). Optothermorheological flow manipulation, *Opt. Lett.* 34: 1976–1978.
URL: *http://ol.osa.org/abstract.cfm?URI=ol-34-13-1976*

Lajeunesse, E. & Homsy, G. M. (2003). Thermocapillary migration of long bubbles in polygonal tubes. II. Experiments, *Phys. Fluids* 15: 308–314.
URL: *http://link.aip.org/link/?PHF/15/308/1*

Link, D. R., Anna, S. L., Weitz, D. A. & Stone, H. A. (2004). Geometrically mediated breakup of drops in microfluidic devices, *Phys. Rev. Lett.* 92: 054503.
URL: *http://link.aps.org/doi/10.1103/PhysRevLett.92.054503*

Liu, G. L., Kim, J., Lu, Y. U. & Lee, L. P. (2006). Optofluidic control using photothermal nanoparticles, *Nature Mater.* 5: 27–32.
URL: *http://dx.doi.org/10.1038/nmat1528*

Marcano, A. O. & Aranguren, L. (1993). Laser-induced force for bubble-trapping in liquids, *Appl. Phys. B: Lasers and Optics* 56: 343–346.
URL: *http://dx.doi.org/10.1007/BF00324530*

Mast, C. B. & Braun, D. (2010). Thermal trap for DNA replication, *Phys. Rev. Lett.* 104: 188102.
URL: *http://link.aps.org/doi/10.1103/PhysRevLett.104.188102*

Mazouchi, A. & Homsy, G. M. (2000). Thermocapillary migration of long bubbles in cylindrical capillary tubes, *Phys. Fluids* 12: 542–549.
URL: *http://link.aip.org/link/?PHF/12/542/1*

Mazouchi, A. & Homsy, G. M. (2001). Thermocapillary migration of long bubbles in polygonal tubes. I. Theory, *Phys. Fluids* 13: 1594–1600.
URL: *http://link.aip.org/link/?PHF/13/1594/1*

Monat, C., Domachuk, P. & Eggleton, B. J. (2007). Integrated optofluidics: A new river of light, *Nature Photon.* 1: 106–114.
URL: *http://dx.doi.org/10.1038/nphoton.2006.96*

Nagy, P. T. & Neitzel, G. P. (2008). Optical levitation and transport of microdroplets: proof of concept, *Phys. Fluids* 20: 101703.
URL: *http://link.aip.org/link/?PHF/20/101703/1*

Ohta, A. T., Jamshidi, A., Valley, J. K., Hsu, H.-Y. & Wu, M. C. (2007). Optically actuated thermocapillary movement of gas bubbles on an absorbing substrate, *Appl. Phys. Lett.* 91: 074103.
URL: *http://link.aip.org/link/?APL/91/074103/1*

Okawa, D., Pastine, S. J., Zettl, A. & Fréchet, J. M. J. (2009). Surface tension mediated conversion of light to work, *J. Am. Chem. Soc.* 131: 5396–5398.
URL: *http://dx.doi.org/10.1021/ja900130n*

Ottino, J. M. & Wiggins, S. (2004). Introduction: mixing in microfluidics, *Phil. Trans. R. Soc. Lond. A* 362: 923–935.
URL: *http://rsta.royalsocietypublishing.org/content/362/1818/923.abstract*

Park, S.-Y., Wu, T.-H., Chen, Y., Teitell, M. A. & Chiou, P.-Y. (2011). High-speed droplet generation on demand driven by pulse laser-induced cavitation, *Lab Chip* 11: 1010–1012.
URL: *http://dx.doi.org/10.1039/C0LC00555J*

Passian, A., Zahrai, S., Lereu, A. L., Farahi, R. H., Ferrell, T. L. & Thundat, T. (2006). Nonradiative surface plasmon assisted microscale Marangoni forces, *Phys. Rev. E* 73: 066311.
URL: *http://link.aps.org/doi/10.1103/PhysRevE.73.066311*

Piazza, R. & Parola, A. (2008). Thermophoresis in colloidal suspensions, *J. Phys.: Condens. Matter* 20: 153102.
URL: *http://stacks.iop.org/0953-8984/20/i=15/a=153102*

Robert de Saint Vincent, M., Wunenburger, R. & Delville, J.-P. (2008). Laser switching and sorting for high speed digital microfluidics, *Appl. Phys. Lett.* 92: 154105.
URL: *http://link.aip.org/link/?APL/92/154105/1*

Rybalko, S., Magome, N. & Yoshikawa, K. (2004). Forward and backward laser-guided motion of an oil droplet, *Phys. Rev. E* 70: 046301.
URL: *http://link.aps.org/doi/10.1103/PhysRevE.70.046301*

Shirasaki, Y., Tanaka, J., Makazu, H., Tashiro, K., Shoji, S., Tsukita, S. & Funatsu, T. (2006). On-chip cell sorting system using laser-induced heating of a thermoreversible gelation polymer to control flow, *Anal. Chem.* 78: 695–701.
URL: *http://dx.doi.org/10.1021/ac0511041*

Song, H., Chen, D. L. & Ismagilov, R. F. (2006). Reactions in droplets in microfluidic channels, *Angew. Chem. Int. Ed.* 45: 7336–7356.
URL: *http://dx.doi.org/10.1002/anie.200601554*

Squires, T. M. & Quake, S. R. (2005). Microfluidics: fluid physics at the nanoliter scale, *Rev. Mod. Phys.* 77: 977–1026.
URL: *http://link.aps.org/doi/10.1103/RevModPhys.77.977*

Stevenson, D. J., Gunn-Moore, F. J., Campbell, P. & Dholakia, K. (2010). Single cell optical transfection, *J. R. Soc. Interface* 7: 863–871.
URL: *http://rsif.royalsocietypublishing.org/content/7/47/863.abstract*

Tan, W.-H. & Takeuchi, S. (2007). A trap-and-release integrated microfluidic system for dynamic microarray applications, *Proc. Natl. Acad. Sci. USA* 104: 1146–1151.
URL: *http://www.pnas.org/content/104/4/1146.abstract*

Tan, W.-H. & Takeuchi, S. (2008). Dynamic microarray system with gentle retrieval mechanism for cell-encapsulating hydrogel beads, *Lab Chip* 8: 259–266.
URL: *http://dx.doi.org/10.1039/B714573J*

Theberge, A. B., Courtois, F., Schaerli, Y., Fischlechner, M., Abell, C., Hollfelder, F. & Huck, W. T. S. (2010). Microdroplets in microfluidics: An evolving platform for discoveries in chemistry and biology, *Angew. Chem. Int. Ed.* 49: 5846–5868.
URL: *http://dx.doi.org/10.1002/anie.200906653*

Verneuil, E., Cordero, M. L., Gallaire, F. & Baroud, C. N. (2009). Laser-induced force on a microfluidic drop: Origin and magnitude, *Langmuir* 25: 5127–5134.
URL: *http://dx.doi.org/10.1021/la8041605*

Vogel, A., Lauterborn, W. & Timm, R. (1989). Optical and acoustic investigations of the dynamics of laser-produced cavitation bubbles near a solid boundary, *J. Fluid Mech.* 206: 299–338.
URL: *http://dx.doi.org/10.1017/S0022112089002314*

Weinert, F. M. & Braun, D. (2008a). Observation of slip flow in thermophoresis, *Phys. Rev. Lett.* 101: 168301.
URL: *http://link.aps.org/doi/10.1103/PhysRevLett.101.168301*

Weinert, F. M. & Braun, D. (2008b). Optically driven fluid flow along arbitrary microscale patterns using thermoviscous expansion, *J. Appl. Phys.* 104: 104701.
URL: *http://link.aip.org/link/?JAP/104/104701/1*

Weinert, F. M. & Braun, D. (2009). An optical conveyor for molecules, *Nano Lett.* 9: 4264–4267.
URL: *http://dx.doi.org/10.1021/nl902503c*

Weinert, F. M., Wühr, M. & Braun, D. (2009). Light driven microflow in ice, *Appl. Phys. Lett.* 94: 113901.
URL: *http://link.aip.org/link/?APL/94/113901/1*

Wienken, C. J., Baaske, P., Rothbauer, U., Braun, D. & Duhr, S. (2010). Protein-binding assays in biological liquids using microscale thermophoresis, *Nat. Commun.* 1: 100.
URL: *http://dx.doi.org/10.1038/ncomms1093*

Würger, A. (2007). Thermophoresis in colloidal suspensions driven by Marangoni forces, *Phys. Rev. Lett.* 98: 138301.
URL: *http://link.aps.org/doi/10.1103/PhysRevLett.98.138301*

Würger, A. (2009). Molecular-weight dependent thermal diffusion in dilute polymer solutions, *Phys. Rev. Lett.* 102: 078302.
URL: *http://link.aps.org/doi/10.1103/PhysRevLett.102.078302*

Würger, A. (2010). Thermal non-equilibrium transport in colloids, *Rep. Prog. Phys.* 73: 126601.
URL: *http://stacks.iop.org/0034-4885/73/i=12/a=126601*

Young, N. O., Goldstein, J. S. & Block, M. J. (1959). The motion of bubbles in a vertical temperature gradient, *J. Fluid Mech.* 6: 350–356.
URL: *http://dx.doi.org/10.1017/S0022112059000684*